IEEE Access
Multidisciplinary | Rapid Review | Open Access Journal

Received December 13, 2018, accepted January 14, 2019, date of publication January 29, 2019, date of current version February 14, 2019.

*Digital Object Identifier 10.1109/ACCESS.2019.2895675*

# A Power Distribution Control Strategy Between Energy Storage Elements and Capacitors for Cascaded Multilevel Inverter With Hybrid Energy Sources

**ZHAO LIU, YUE ZHANG, SHANSHAN ZHAO, AND JIAN GONG**
School of Automation, Nanjing University of Science and Technology, Nanjing 210094, China

Corresponding author: Zhao Liu (liuzhao@njust.edu.cn)

This work was supported in part by the National Natural Science Foundation of China under Grant 51507086, and in part by the Natural Science Foundation of Jiangsu Province under Grant BK20150839.

**ABSTRACT** The key technology of a cascaded multilevel inverter with hybrid energy sources lies in the power distribution among different chains. A power distribution control strategy between the energy storage elements and the capacitors is proposed to achieve fault tolerant control. In the cascaded multilevel inverter with hybrid energy sources, the chains with energy storage elements can operate in four quadrants, while the chains with capacitors can only operate in two quadrants. With the proposed control method, the active power distribution is realized by active voltage vector superposition, and the reactive power distribution is achieved by initial operation point selection. This enhances both the system reliability and availability while enabling continuous operation in four quadrants. Meanwhile, the stable operation region and the range of the initial operating point have been derived by the vector analysis to avoid over-modulation. An experimental prototype based on a single-phase link with two series chains has been built in the laboratory. The simulation and experimental results are provided to demonstrate the effectiveness of the proposed control method.

**INDEX TERMS** DC-AC power converters, power control, voltage control, energy conversion, energy exchange, energy storage, power generation control.

## I. INTRODUCTION

Over the last decade, renewable energy sources such as photovoltaics and wind-power generation have been progressively installed within distribution power systems. However, the output power of photovoltaics and wind-power generation depends on weather and climate conditions significantly. Electric power utilities may face system stability issues, which are related to voltage and frequency fluctuations resulting from the intermittent nature of renewable energy sources. Energy storage helps to mitigate the stochastic nature of renewable resources. In addition, energy storage can quickly deliver active power to provide services, such as spinning reserve, peak shaving, load levelling, and load frequency control [1]–[3]. Compared to other energy storage system, battery energy storage system (BESS) has been proved more attractive for its fast reaction and high power density. A BESS installation has two major hardware components: a power conversion system (PCS) and a network of battery energy storage units [4]. A comparison among a conventional design using parallel power blocks (PBBESS), a design using intelligent battery packs (IBP-BESS) and a cascaded H-bridge design (CHB-BESS) has been given in reference [5], cascaded multilevel inverter has the characteristics that it could be connected with medium-voltage grid directly without transformer and its capacity could be expanded easily, so it is widely used as the PCS of BESS [6], [7]. Beyond offering above significant benefits, the cascaded BESS suffers from the drawback of employing great number of components, which will lead to reduction in the reliability.

The so-called ''fault tolerance'' for cascaded multilevel inverter has been investigated in [8]–[12]. For a cascaded converter, fault-tolerant control can be achieved by two ways [8]:

1) by providing a redundant converter cell in each phase, and bypassing not only the faulty converter cell, but also two healthy converter cells in the other two phases;

The associate editor coordinating the review of this manuscript and approving it for publication was Bora Onat.

2) by bypassing the faulty converter cell only, without providing redundant converter cells.

The first category can ride through a fault in at least one converter cell at the rated voltage and power. Reference [9] proposes a fault-tolerant control strategy to achieve the N+1 redundancy in a cascaded H-bridge multilevel converter (CHMC) based STATCOM system and redundant H-bridge building block (HBBB) is designed and applied to deal with the switching device failure and improve the reliability and availability. In [10], a method for fault-tolerant operation of three phase CHB converters was presented, which employs an auxiliary module made by six semiconductor switches and one capacitor in series to the CHB converter. This category of approaches is often used in critical applications at the expense of cost and efficiency. The second category can tolerate a fault in a few converter cells with a reduced voltage and power. Reference [11] has proposed a modified level-shifted pulse width modulation (LS-PWM) strategy to apply the neutral shift for fault-tolerant control of cascaded H bridge multilevel inverters (CHMIs). When the proposed LS-PWM is applied with the neutral shift, the cascaded multilevel inverter can maintain continuous operation, producing three-phase balanced line-to-line voltages and currents at the ac side during a switching device fault. The proposed fault-tolerant strategy in [12] is based on an adaptation of the modified space vector modulation (SVM) technique to the fundamental phase-shift compensation method, and it generates balanced line-to-line voltages with increased voltage levels in the faulty condition. Although a tolerable degree of reduction in voltage and power depends on the application, it is acceptable in terms of avoiding the complete shutdown in most cases. The parallel connection is required for the battery strings, each of which consists of series-connected battery modules. Thus, desirable power and energy ratings can be obtained by connecting multiple battery strings in parallel. However, parallel and series connections of many battery modules inherently bring complexity to the battery management system (BMS) [3], and too many batteries and BMS are prone to failure. The battery consistency, overvoltage, overheating, and BMS communication failure can cause the fault, either of the above two methods will cause voltage and power loss if the batteries/BMS fail. Actually, the fault batteries/BMS can be removed by switching off the contactors to form cascaded multilevel inverter with hybrid energy sources, the battery and the capacitor serve as two main DC sources, shown in Fig.1.

The cascaded multilevel inverter with hybrid energy source have been widely studied and applied. The key lies in the power distribution among different chains. In [13], a way based on a time-domain modulation strategy is presented, it can achieve any dc voltage ratio between the H-bridges of the single-dc-source cascaded H-bridge converter. In [14], using the phase-shift modulation approach, a new control method for cascaded H-bridge multilevel converters fed with only one independent dc source is presented. The proposed method has a wide voltage regulation range for the

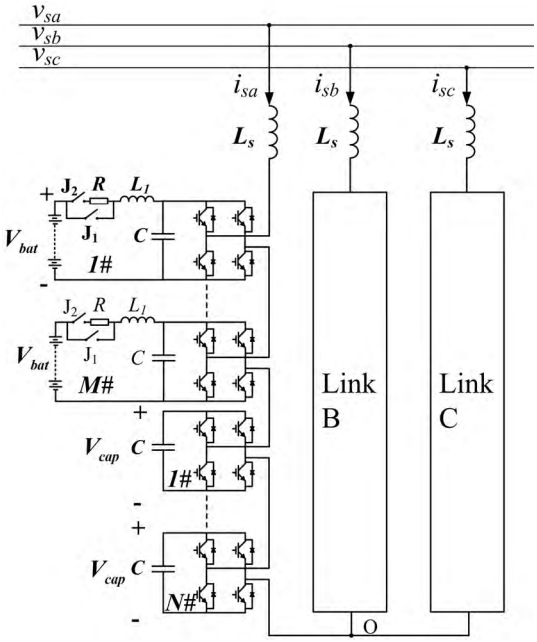


**FIGURE 1.** Star-connected cascaded multilevel inverter with hybrid energy sources.

replacement capacitors in the H-bridge cells. A segmented power-distribution control system based on a hybrid cascaded multilevel converter with parts of energy storage is proposed in [15], a novel three-segmented control strategy based on active and reactive power control is proposed to realize the energy flow among the ordinary cells, storage cells, and the motor. A power-distribution strategy between the energy source, the energy storage, and the electric motor has been developed and implemented in [16], an autonomous power regenerative control has been proposed to achieve the voltage balancing control of the energy storage. However, the above methods are all controlled as voltage source converter (VSC), it is not suitable for grid-connected inverter. The control strategy of grid-connected asymmetrical cascaded multilevel converter has been considered in [17], the battery and the electrical double layer capacitor (EDLC) serve as dc sources, and feed forward space vector modulation technique (FFSVM) is used to distribute active power between battery and EDLCs. With the proposed voltage feed-forward mechanism, the hybrid energy storage system can flexibly operate in different modes, but it cannot regulate the active and reactive power continuously. Furthermore, the distribution of reactive power among chains is not considered. Traditionally, the decoupled active and reactive power distribution control is adopted in cascaded multilevel inverter with hybrid energy sources. A CHB inverter topology with both PV arrays and energy storage elements is proposed in [18], and a two-layer hierarchical control is also developed. The lower layer is responsible for system PQ control and distribution among each HB, and the upper layer decides power dispatching and generate power references for each H-bridge (HB). However, there is a delay in the active and reactive decoupling

separation, so its dynamic response is slow and the chains may also be over modulated during the dynamic process.

This paper proposes a power distribution control method for cascaded multilevel inverter with hybrid energy sources. In particular, the active power distribution between the energy storage elements and the capacitors is realized by active voltage vector superposition, and the reactive power distribution is achieved by initial operation point selection. Moreover, the selection range of initial operation point is described in detail in this paper, which can avoid over-modulation. To enhance both system reliability and redundancy, the stable operation region also has been derived by vector analysis. Accordingly, the proposed power distribution control method will not only make full utilization of the system's capacity but also enable continuous operation in four quadrants, it can be used not only in the occasion of batteries and capacitors to achieve fault-tolerant control but also in other occasions with hybrid energy source such as batteries and PV, batteries and EDLCs and so on.

This paper is outlined as follows. After the introduction section, a simplified equivalent model is given and the operation modes are described in Section II. An insightful illustration of the proposed power distribution strategy between the energy storage and the capacitors is shown in Section III. The range of initial operation point is also derived in this section to avoid over-modulation. Section IV presents the stable operation range of cascaded multilevel inverter with hybrid energy sources by vector analysis. In Section V and Section VI, the proposed system is firstly simulated in a MATLAB/Simulink simulation platform and then implemented on an experimental prototype based on a single phase link with two series chains. Simulation and experimental results are presented to verify the effectiveness of the proposed control method. Finally, conclusions are presented in Section VII.

## II. EQUIVALENT MODEL OF SYSTEM

According to [19] and [20], either star-connected or delta-connected cascaded multilevel inverter can be divided into three single-phase links by individual control, so taking an arbitrary link in Fig.1 as study object, which is shown in Fig.2. It can be assumed that there are $M$-chains with batteries and $N$-chains with capacitors in the link. Where $v_s$ is the grid voltage, $i_s$ is the grid current, $V_{cap}$ and $V_{bat}$ are respectively the DC voltages, $L_s$ is the filter inductor, which ignores the resistor. A pre-charge circuit is formed by $R$, $J_1$ and $J_2$, $L_1$ is used to reduce the second harmonic current. By the methods proposed in [21] and [22], all chains with batteries and all chains with capacitors can respectively be assumed to the same.

To simplify the analysis, the link can be equivalent to two series chains, as shown in Fig.3. Where $v_{r1}$ is the output voltage of chains with batteries, $v_{r2}$ is the output voltage of chains with capacitors, $v_L$ is the inductor voltage.

$v_{r1}$, $v_{r2}$ and $v_L$ are consisted of fundamental voltage and harmonic voltage. Usually the phase-shift SPWM modulation

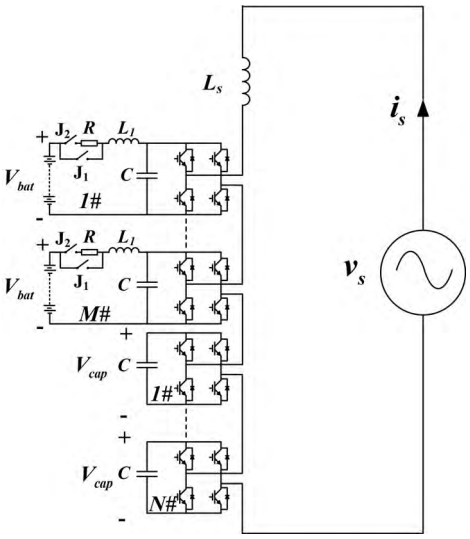


**FIGURE 2.** The single-phase link.

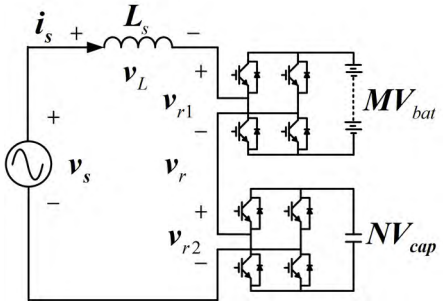


**FIGURE 3.** The equivalent circuit of single-phase link.

is adopted in cascaded multilevel inverter and it will not be over modulated, the harmonic voltages are mainly switching frequency harmonic and are relatively small, so they can be ignored.

Thus:

$$\boldsymbol{v_s} = \boldsymbol{v_r} + \boldsymbol{j}\omega L_s \cdot \boldsymbol{i_s} = \boldsymbol{v_{r1}} + \boldsymbol{v_{r2}} + \boldsymbol{j}\omega L_s \cdot \boldsymbol{i_s} \tag{1}$$

where:

$$\begin{cases} v_s = V_s \angle 0 \\ v_{r1} = V_{r1} \angle \varphi_3 \\ v_{r2} = V_{r2} \angle \varphi_4 \\ V_{r1} = M_a \cdot V_{r1m} = M_a \cdot MV_{bat}/\sqrt{2} \\ V_{r2} = M_b \cdot V_{r2m} = M_b \cdot NV_{cap}/\sqrt{2} \end{cases} \tag{2}$$

The grid voltage $v_s$ is chosen as the phase reference and its RMS is $V_s$; $V_{r1}$ and $\varphi_3$ are respectively the RMS and phase of $v_{r1}$; $V_{r2}$ and $\varphi_4$ are respectively the RMS and phase of $v_{r2}$; $V_{r1m}$ and $V_{r2m}$ are respectively the maximum of $V_{r1}$ and $V_{r2}$; $M_a$ and $M_b$ are respectively the modulation ratio, and $0 \le M_a \le 1, 0 \le M_b \le 1$.

The cascaded multilevel inverter with hybrid energy sources can operate in four quadrants, and the vector diagrams of operation mode are shown in Fig.4. Where $\delta$ is the

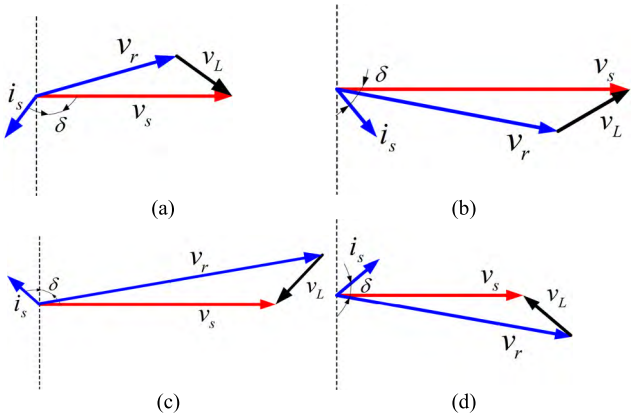


**FIGURE 4.** The vector diagrams of operation mode. (a) Quadrant three. (b) Quadrant four. (c) Quadrant two. (d) Quadrant one.

angle between $v_r$ and $i_s$, and it also denotes the power factor of the hybrid energy storage system.

The operation modes in Fig.4 can be divided into two categories, the operation modes of Fig.4(a) and Fig.4(b) are similar and can be defined as inductive mode while the operation modes of Fig.4(c) and Fig.4(d) can be defined as capacitive mode.

## III. PROPOSED CONTROL METHOD

In Fig.3, the chain with batteries can operate in four quadrants while the chain with capacitors can only operate in two quadrants. Ideally the chain with capacitors cannot absorb active power, but because there is power loss in the chain, including DC-side power loss, switching loss, and so on, it needs to absorb a little active power to cancel out the loss. The aim of active power distribution is that the batteries provide all active power and the capacitors absorb a little active power to maintain its DC-side voltages.

Taking the inductive mode in Fig.4(a) for example, since the other modes have the similar analyzing methods and conclusions. The vector diagram is shown in the Fig.5. CC1 is a circle centered on point $O_1$ and its radius is $V_{r1m}$. By formula (2), arbitrary vector in CC1 can be obtained by changing the modulation ratio $M_a$ and phase angle $\varphi_3$ of $v_{r1}$, so CC1 represents the output voltage range of $v_{r1}$ without over-modulation. Similarly, CC2 is a circle centered on point $O_2$ and its radius is $V_{r2m}$, which represents the output voltage range of $v_{r2}$ without over-modulation. The black shadow area P is the overlapping part of CC1 and CC2, which means that the steady-state operating point can only be synthesized in this area, for only in this area vector $v_{r1}$ and vector $v_{r2}$ can synthesis vector $v_r$ without over-modulation.

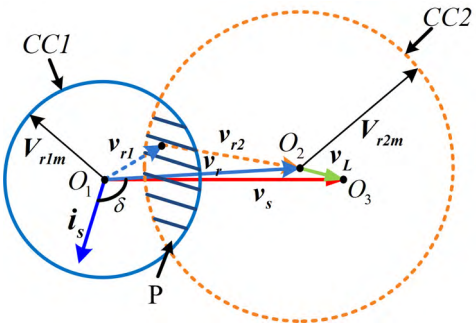


**FIGURE 5.** The vector diagrams in inductive mode.

The power loss of chain with capacitors is small and can be neglected, so $v_{r2}$ must be perpendicular to $i_s$, which is shown in Fig.6. The $A_1A_2$ is the line segment where $v_{r2}$ and area P intersect, which means that the steady-state operating point can only be located at this line segment.

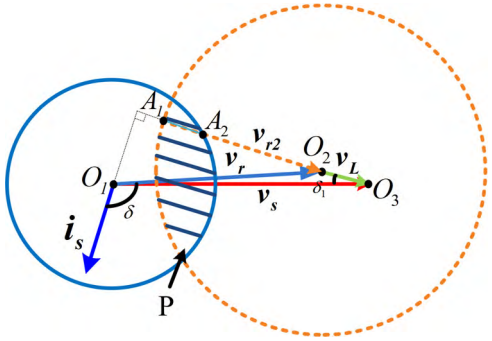


**FIGURE 6.** The stable operation region in inductive mode.

According to the balance control proposed in literature [3], the initial operation point is located at point B, and $O_1B{:}O_2B{=}MV_{bat}{:}NV_{cap}$, which is shown in Fig.7, then a vector parallel with $i_s$ which can be called "the active power voltage vector" is added based on the point B.

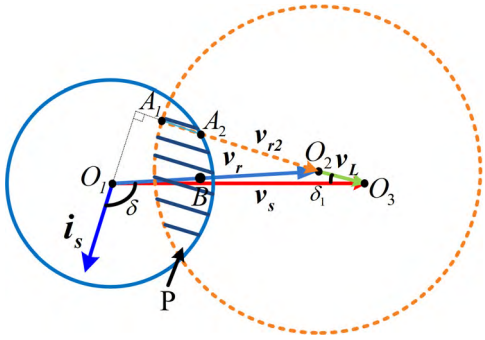


**FIGURE 7.** The initial operation point.

But it can be known from Fig.7 that it is difficult to find appropriate active power voltage vector which makes the point B transition to $A_1A_2$, so the initial operation point can be adjusted, shown in the Fig.8. Two lines parallel to $i_s$ have been given from points $A_1$ and $A_2$ respectively, and the parallel lines intersect $v_r$ at points $B_1$ and $B_2$ respectively. The initial operation point B can be selected on the line segment $B_1B_2$, and it is easy to find appropriate active power voltage vector to make point B transition to point A.

The control block diagram is proposed in Fig.9. The proposed control method is consisted of five parts, including active and reactive power control, initial operation

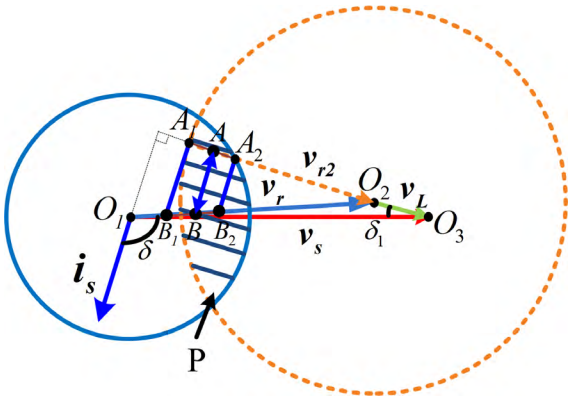


**FIGURE 8.** The range of initial operation point.

point selection, active power distribution control, balance control and SPWM modulation.

In the active and reactive power control, the reference current is consisted of active and reactive current, a PI controller is adopted to track the reference current, the $k_{p1}$ and $k_{i1}$ are designed to ensure good steady-state and dynamic performance, the grid voltage is feedforward by coefficient $k$. Firstly, the demanded active and reactive power is controlled by the current-loop, then it can be distributed respectively.

The output of current-loop control is divided into two parts based on the position of initial operation point, one part is as the output voltage vector of chains with batteries while the other part is as that of chains with capacitors. Where m=$O_1B/O_1O_2$, which represents the position of the initial operation point. The selection of m depends on the reactive power distribution between two parts.

The active power needs to be distributed between the batteries and the capacitors. As discussed above, the chains with capacitors absorb active power to maintain its DC-voltage, so an active voltage vector is added to its output voltage, the active voltage vector is generated by the closed loop of DC capacitor voltage and it is parallel with $i_s$, the reference voltage is the sum of capacitor voltages and the feedback is the actual value. When the actual voltage is lower than the reference, a vector with the same direction of phase current is superimposed, vice versa a vector with the opposite direction is superimposed. At the same time, this active voltage vector is subtracted from the output voltage of chains with batteries. So:

$$\begin{cases} v_{r1} = mv_r - (NV^*_{cap} - NV_{cap}) \cdot (k_{p2} + \dfrac{k_{i2}}{s}) \cdot i^*_s \\ v_{r2} = (1-m)v_r + (NV^*_{cap} - NV_{cap}) \cdot (k_{p2} + \dfrac{k_{i2}}{s}) \cdot i^*_s \end{cases} \tag{3}$$

By formula (3), $v_{r1}$ and $v_{r2}$ can still synthesis $v_r$, it's proved that the power distribution control will not affect the active and reactive power control and they are absolutely decoupled, so the proposed control method is with good stability and the controller parameters are simple to design.

The proposed control method can achieve power distribution between the batteries and the capacitors, but there are differences among chains, so all the chains need to be balanced. The balance control including SOC balance control and voltage balance control has been discussed in detail in [19] and [20], and it has been widely used, so it doesn't need to be discussed in this paper and all chains are assumed to be the same.

The output of balance control is as the modulation wave of each chain, the phase-shift SPWM modulation is adopted to generate PWM drive.

It is necessary to derive the range of m to avoid over-modulation. When the initial operation point is located at point $B_1$, the vector diagram is shown in Fig.10. Where $\delta_1$ is the angle between $v_L$ and $v_s$, $\delta_2$ is the angle between $v_r$ and $v_L$, $\varphi_1$ is the angle between $v_{r2}$ and $v_r$.

$$m_{B1} = 1 - \frac{\overrightarrow{o_2B_1}}{\overrightarrow{o_1o_2}} = 1 - \frac{V_{r2m}}{V_r \cos\varphi_1} \tag{4}$$

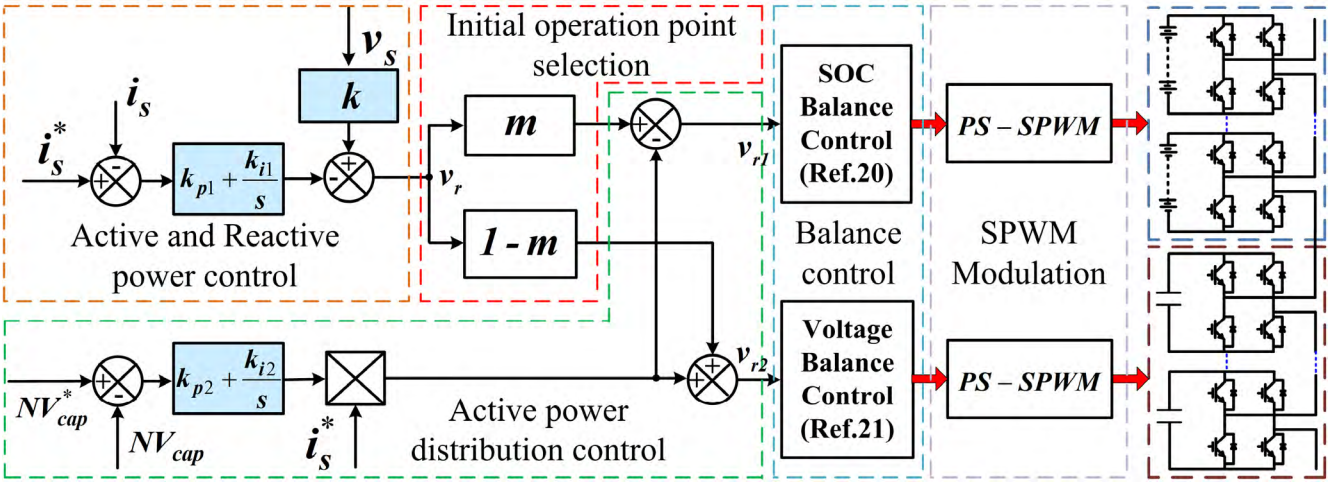


**FIGURE 9.** The control diagram of proposed method.

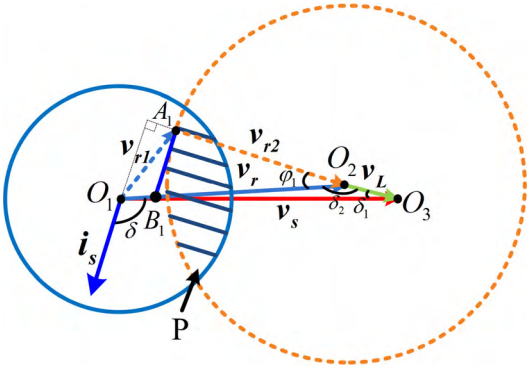


**FIGURE 10.** The calculation of m when the initial operation point is at point $B_1$.

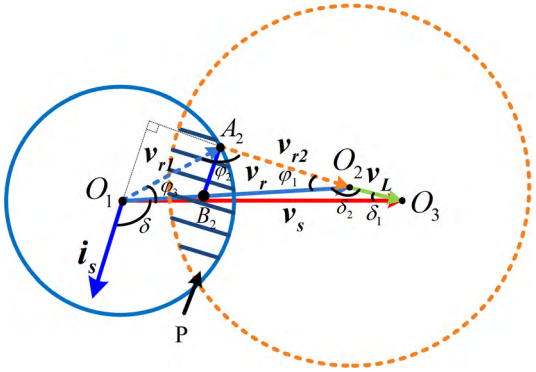


**FIGURE 11.** The calculation of m when the initial operation point is at point $B_2$.

where:

$$\begin{cases} \delta_1 = \delta - \dfrac{\pi}{2} \\ V_r = \sqrt{V_s^2 + V_L^2 - 2 \cdot V_s \cdot V_L \cdot \cos\delta_1} \\ \cos\varphi_1 = -\cos\delta_2 = \dfrac{V_s^2 - V_r^2 - V_L^2}{2 \cdot V_r \cdot V_L} \\ V_{r2m} = \dfrac{NV_{cap}}{\sqrt{2}} \end{cases} \tag{5}$$

Similarly, when the initial operation point is located at point $B_2$, the vector diagram is shown in Fig.11. Where $\varphi_2$ is the angle between $v_{r1}$ and $v_{r2}$, $\varphi_3$ is the angle between $v_{r1}$ and $v_s$.

$$\boldsymbol{m_{B2}} = 1 - \frac{\overrightarrow{\boldsymbol{o_2 B_2}}}{\overrightarrow{\boldsymbol{o_1 o_2}}} = 1 - \frac{\boldsymbol{V_{r2}}}{\boldsymbol{V_r}\cos\varphi_1} \tag{6}$$

where:

$$\begin{cases} \delta_1 = \delta - \dfrac{\pi}{2} \\ V_r = \sqrt{V_s^2 + V_L^2 - 2 \cdot V_s \cdot V_L \cdot \cos\delta_1} \\ \cos\varphi_1 = -\cos\delta_2 = \dfrac{V_s^2 - V_r^2 - V_L^2}{2 \cdot V_r \cdot V_L} \\ V_{r1m} = \dfrac{MV_{bat}}{\sqrt{2}} \\ \varphi_2 = \pi - \arcsin(\dfrac{V_s}{V_{r1m}} \cdot \sin\delta_1) \\ \varphi_3 = \pi - \varphi_2 - \delta_1 = \arcsin(\dfrac{V_s}{V_{r1m}} \cdot \sin\delta_1) - \delta_1 \\ V_{r2} = \dfrac{\sin\varphi_3}{\sin\delta_1} \cdot V_{r1m} - V_L \end{cases} \tag{7}$$

The initial operation point B is located on the line segment $B_1B_2$, so

$$\boldsymbol{m} \in \begin{bmatrix} \boldsymbol{m_{B1}} & \boldsymbol{m_{B2}} \end{bmatrix}$$

The selection of m depends on the distribution of reactive power between two chains.

When the hybrid energy storage system operates in capacitive mode, the range of initial operation point is shown in Fig.12. Similarly, the range of m can be also derived by geometric analysis.

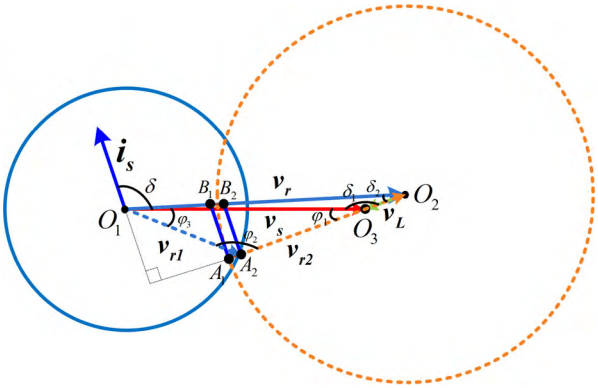


**FIGURE 12.** The range of initial operation point in capacitive mode.

## IV. STABLE OPERATION RANGE ANALYSIS

When the hybrid energy storage system operates in inductive mode, it can be known from Fig.6 that $v_{r2}$ must intersect area $P$ to avoid over-modulation of the system, so it is needed to meet the following two conditions in Fig.13. Where $\gamma$ is the angle between $O_2O$ and $v_r$.

1) The triangle $O_1O_2A_2$ needs to be within the triangle $O_1O_2O$, which means $\varphi_1 < \gamma$.

2) The triangle $O_1O_2O_3$ can be constructed, which means $\cos\delta_1 \leq 1$.

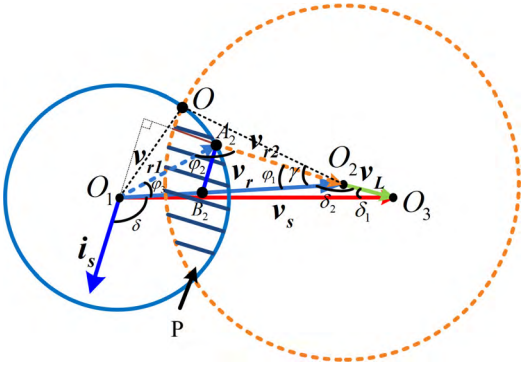


**FIGURE 13.** The operation region of hybrid energy storage system in inductive mode.

(a) $\varphi_1 < \gamma$
Then it can be concluded that:

$$\begin{cases} \cos\varphi_1 = -\cos\delta_2 = -\dfrac{V_r^2 + V_L^2 - V_s^2}{2V_rV_L} \\ \cos\gamma = \dfrac{V_r^2 + V_{r2m}^2 - V_{r1m}^2}{2V_rV_{r2m}} \\ \cos\varphi_1 > \cos\gamma \end{cases} \tag{8}$$

So,

$$Vr < \sqrt{\frac{V_L \cdot (V_{r1m}^2 - V_{r2m}^2) + V_{r2m} \cdot (V_s^2 - V_L^2)}{V_L + V_{r2m}}} \tag{9}$$

(b) $\cos\delta_1 \leq 1$
Where,

$$\cos\delta_1 = \frac{V_s^2 + V_L^2 - V_r^2}{2V_sV_L} \tag{10}$$

So,

$$V_r \geq \sqrt{V_s^2 + V_L^2 - 2V_s \cdot V_L} \tag{11}$$

So the range of $V_r$ can be derived by (9) and (11), then the ranges of $\delta$ and $\delta_1$ also can be derived by (10) and (12).

$$\delta = \delta_1 + \frac{\pi}{2} \tag{12}$$

When the hybrid energy storage system operates in capacitive mode, the operation range can be derived similarly according to Fig.14.

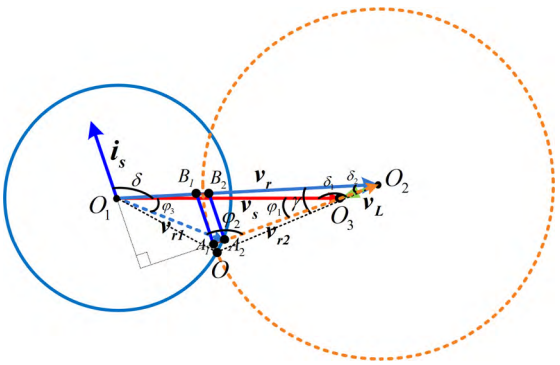


**FIGURE 14.** The operation region of hybrid energy storage system in capacitive mode.

## V. SIMULATION

### A. THE PARAMETERS OF SIMULATION SYSTEM

In order to verify the proposed theoretical analysis, the model of cascaded multilevel inverter with hybrid energy sources controlled by the proposed strategy is simulated with MATLAB/SIMULINK. The simulation is based on a single phase link with two series chains as shown in Fig.3, one chain is with battery as DC source and the other is with capacitor. This paper focuses on the power distribution between energy storage elements and capacitors, so two chains are enough. The detailed parameters are listed in Table 1.

**TABLE 1.** Main parameters of cascaded multilevel inverter with hybrid energy sources.

| Parameters | Symbol | Value |
|---|---|---|
| Chain with Batteries | | |
| Nominal voltage | $V_{bat}$ | 100V |
| chain number | $M$ | 1 |
| Chain with Capacitors | | |
| Nominal voltage | $V_{cap}$ | 200V |
| DC capacitor | $C$ | 4200uF |
| Chain number | $N$ | 1 |
| AC side | | |
| Nominal line-ground voltage | $V_s$ | 180V |
| AC inductor | $L_s$ | 1.6mH |
| Switching frequency | $f_s$ | 6kHz |
| Reference current | $I_{qref}$ | 20A |

The simulation is still based on the inductive mode shown in Fig.5. According to the system parameters, there are:

$$\begin{cases} V_{r1m} = \dfrac{MV_{bat}}{\sqrt{2}} = 70.7V \\ V_{r2m} = \dfrac{NV_{cap}}{\sqrt{2}} = 141.4V \\ V_s = 180V \\ V_L = I_s \cdot \omega L_s = 10.1V \end{cases} \tag{13}$$

It can be concluded from formulas (9), (10) and (11), then

$$\begin{cases} V_r \in \left[\, 169.9469V \quad 170.7624V \,\right] \\ \delta_1 \in \left[\, 0 \quad 0.3944 \,\right] \end{cases} \tag{14}$$

When $\delta_1 = 0$, the range of m can be obtained from formulas (4) and (6), that:

$$m \in \left[\, 0.1678 \quad 0.6431 \,\right] \tag{15}$$

When $\delta_1 = 0.3944$, the range of m can be obtained from (4) and (6), that:

$$m = 0.0942 \tag{16}$$

By formulas (15) and (16), it is proved that $v_{r2}$ intersects area $P$ within the range of $\delta_1$.

Let $\delta_1 = \pi/12$, the range of m can be obtained from formulas (4) and (6), that:

$$m \in \left[\, 0.0844 \quad 0.3556 \,\right] \tag{17}$$

Simulation has been given respectively when m=0.2, 0.4 and 0.6. The simulation is based on the proposed control method in Fig.9 without consideration of balance control. All the active power is provided by chain with batteries, while the chain with capacitors absorbs a little active power to maintain its DC voltage, the reactive power is distributed by initial operation point if it is not over modulated.

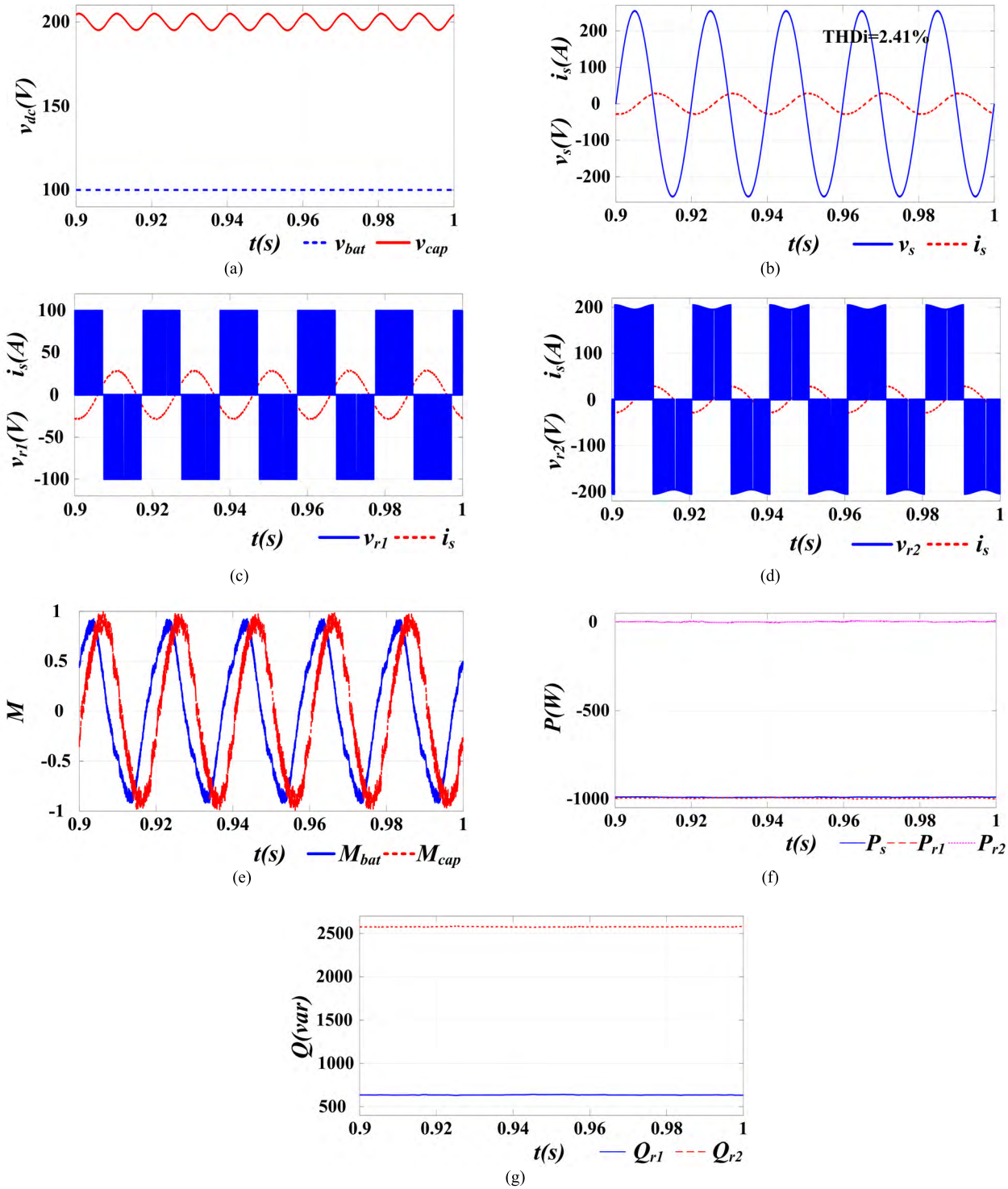


**FIGURE 15.** The simulation when m=0.2, $\delta_1 = \pi/12$. (a) Voltages of battery and capacitor. (b) Grid voltage and current. (c) The output voltage and current of chain with battery. (d) The output voltage and current of chain with capacitor. (e) The modulation waves of different chains. (f) The active power waveforms of grid and different chains. (g) The reactive power of different chains.

### *B. SIMULATION WHEN m=0.2*

Fig.15 shows the simulation results of cascaded multilevel inverter with hybrid energy sources when m=0.2. By formula (17), it is not over modulated. The dc voltage waveforms of the battery and the capacitor are shown in Fig.15(a). The capacitor voltage can be well controlled as 200V, and there is 100Hz ripple voltage in the capacitor voltage. Fig.15(b) shows the grid current and grid voltage, the system operates

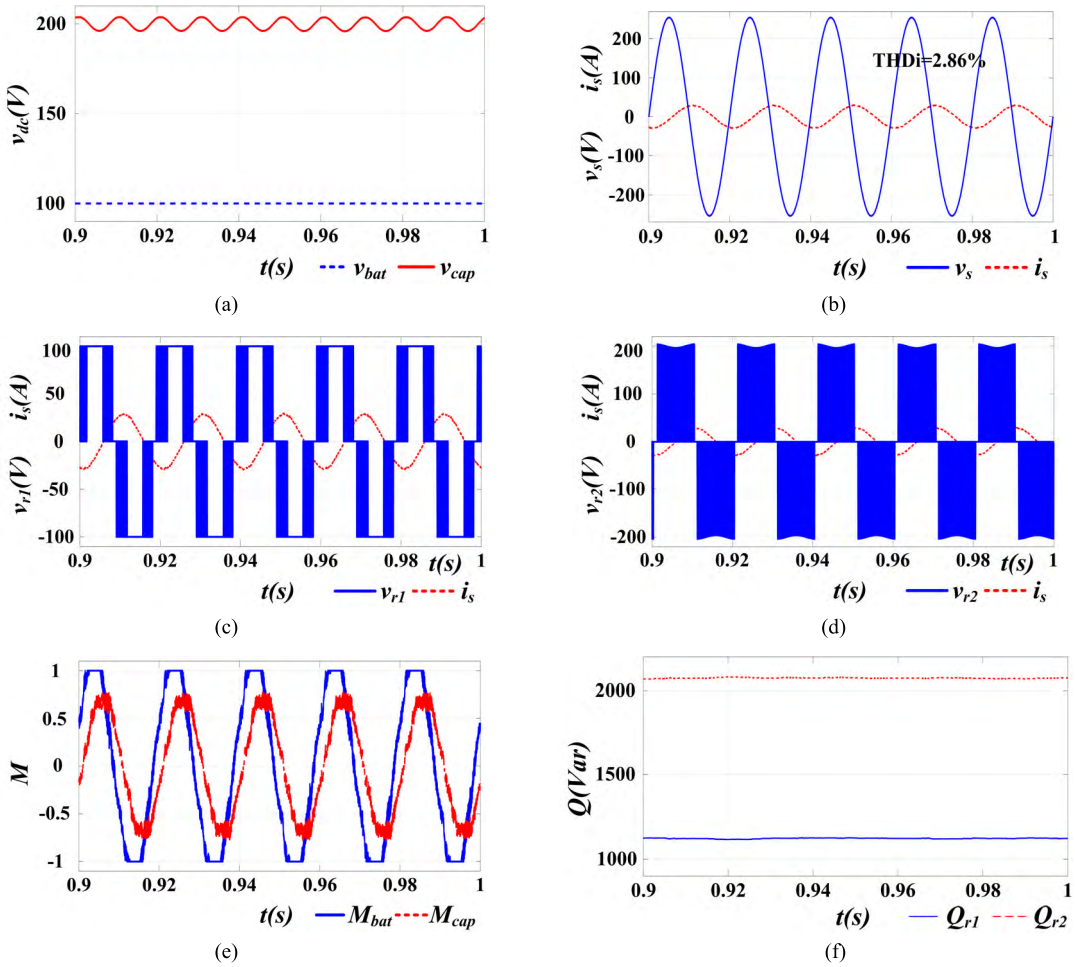


**FIGURE 16.** The simulation when m=0.4, $\delta_1 = \pi/12$. (a) Voltages of battery and capacitor. (b) Grid voltage and current. (c) The output voltage and current of chain with battery. (d) The output voltage and current of chain with capacitor. (e) The modulation waves of different chains. (f) The reactive power of different chains.

in inductive mode, the grid current THD is 2.41%. It can be seen from Fig.15(c) that the chain with battery outputs active power and inductive reactive power. From Fig.15(d) that the current lags the output voltage, so the chain with capacitor outputs inductive reactive power and it needs to absorb active power to maintain its DC voltage. Fig.15(e) shows the modulation waves of both chains, both of the modulation waves are less than 1 and the system is in normal modulation. In Fig.15(f), $P_s$ is the active power provided by grid, $P_{r1}$ and $P_{r2}$ are respectively the active power absorbed by chain with batteries and chain with capacitors, $P_{r1} \approx P_s = -1000$W, $P_{r2} \approx 0$, so the chain with batteries provides all the active power to the grid. In Fig.15(g), $Q_{r1}$ and $Q_{r2}$ are respectively the reactive power provided by chain with batteries and chain with capacitors, $Q_{r1} = 635$var, $Q_{r2} = 2575$var, $Q_{r1}$:$Q_{r2} = 1{:}4.0551 \approx 0.2{:}0.8$, so the reactive power is exactly distributed by initial operation point.

### C. SIMULATION WHEN m=0.4

Fig.16 shows the simulation results of cascaded multilevel inverter with hybrid energy sources when m=0.4. By formula (17), it is out of the range. The simulation results are the same to that of m=0.2, but the grid current is 2.86% and it is over modulated. In Fig.16(f), $Q_{r1} = 1123$var, $Q_{r2} = 2072$var, $Q_{r1}$:$Q_{r2} = 1{:}1.8451 \neq 0.4{:}0.6$, the reactive power distribution is not determined by initial operation point, because the chain with batteries is over modulated.

### D. SIMULATION WHEN m=0.6

Fig.17 shows the simulation results of cascaded multilevel inverter with hybrid energy sources when m=0.6. By formula (17), it is out of the range. In Fig.17 the grid current THD is up to 7.57% and it is over modulated too. In Fig.17(f), $Q_{r1} = 1425$var, $Q_{r2} = 1740$var, $Q_{r1}$:$Q_{r2} = 1{:}1.2211 \neq 0.6{:}0.4$, the reactive power distribution is not determined by initial operation point, because the chain with batteries is over modulated. A comparison has been made among Fig.15, Fig.16 and Fig.17 that the active and reactive power can be controlled by the proposed control method, the active power is distributed properly to maintain the capacitor voltage while the reactive power is distributed based on the initial

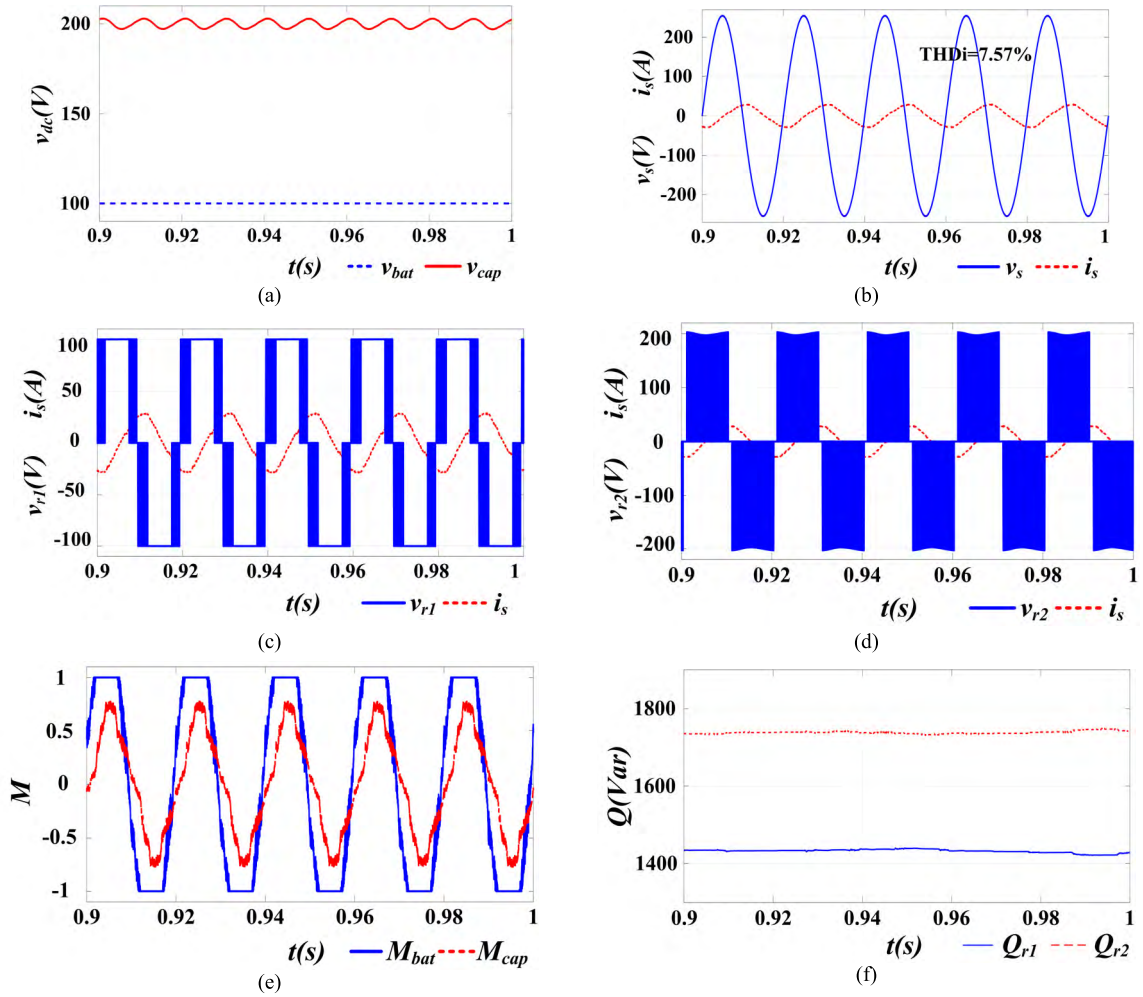


**FIGURE 17.** The simulation when m=0.6, $\delta_1 = \pi/12$. (a) Voltages of battery and capacitor. (b) Grid voltage and current. (c) The output voltage and current of chain with battery. (d) The output voltage and current of chain with capacitor. (e) The modulation waves of different chains. (f) The reactive power of different chains.

operation point if without over-modulation. The correctness of theoretical analysis has been proved.

## VI. EXPERIMENTAL RESULTS

A prototype of cascaded multilevel inverter with hybrid energy sources has been developed to verify the proposed control strategy. The prototype is a single phase link with four series chains, but only two chains are used for experimental verification. The DC source of one chain is a 1000V/40A high precision programmable DC power supply, and the other chain is with capacitor. All the parameters of experimental prototype are the same as that of simulation, which are listed in Table 1. Fig.18 shows the main circuit, single chain and controller of the prototype. The IGBT module is FF300R12ME4, each chain has two IGBT modules, and the IGBT driver is 2SP0115 produced by Concept. The controller is based on single data signal processing (DSP) TM320F28335 and dual complex programmable logic device (CPLD) EPM570T144I5. The DSP is dedicated to realize the proposed control method, one CPLD is used for synchronous sampling, and the other is used for protection and IO control. The controller connects to the chains by optical fibers.


**FIGURE 18.** Experimental prototype.

To avoid over-modulation, only the experimental results when m=0.2 and $\delta_1 = \pi/12$ has been given, shown in Fig.19. Fig.19 (a) shows the output voltage of chain with DC power supply and the grid current, the chain outputs active power and inductive reactive power; Fig.19 (b) shows the output voltage of chain with capacitor and the grid current, the chain outputs inductive reactive power and absorbs a little active power to maintain the DC voltage; Fig.19 (c) shows the grid voltage and grid current, the hybrid energy storage system outputs active power and inductive reactive power; Fig.19 (d) shows the DC capacitor voltage and the voltage of DC power supply, there is second harmonic in the DC capacitor voltage. The experimental results are consistent with those of simulation results. It is shown in Fig.19 that the grid current and capacitor voltage have been well controlled.

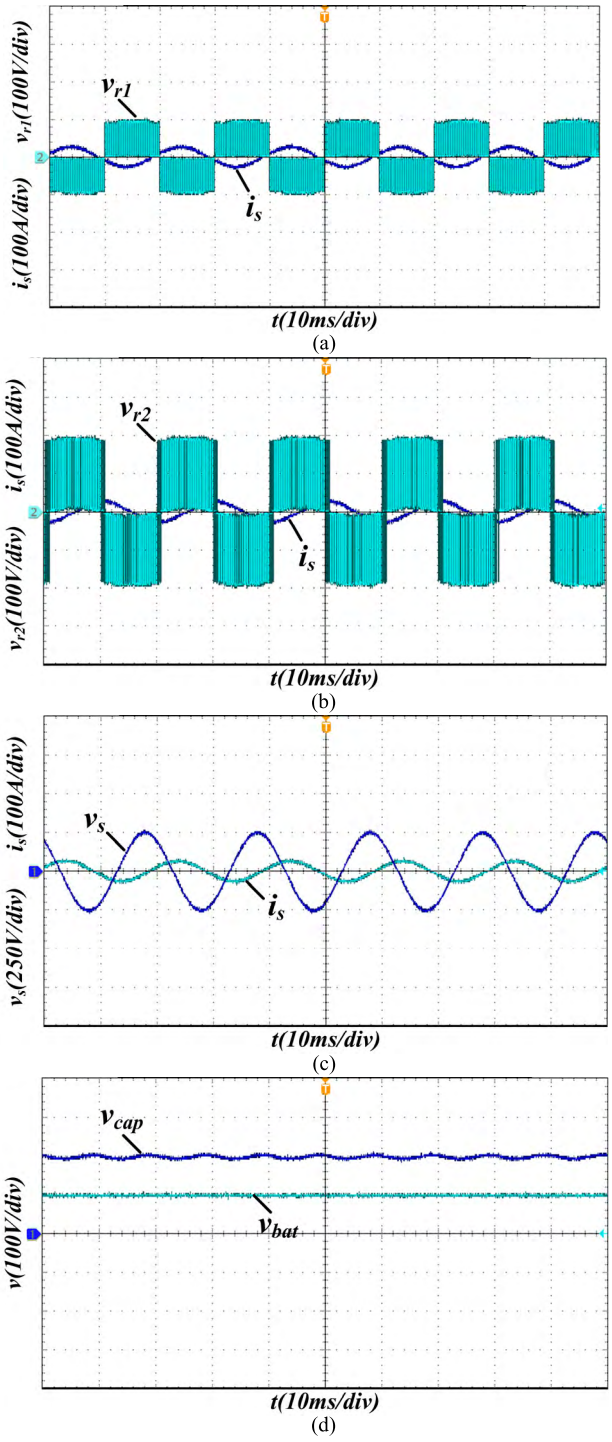


**FIGURE 19.** The experiment when m=0.2, $\delta_1 = \pi/12$. (a) Output voltage and current of chain with DC source versus time. (b) Output voltage and current of chain with capacitor versus time. (c) Grid voltage and current versus time. (d) DC voltages of DC source and capacitor versus time.

The active and reactive power of each chain have been given in Table 2 with power analysis. The reactive power $Q_{r1}$:$Q_{r2}$ = 1:4.09≈1:4. The effectiveness and feasibility of proposed control method have been proved by experiment.

**TABLE 2.** The active and reactive power of each chain in experiment.

| Parameters | Symbol | Value |
|---|---|---|
| Chain with DC source | | |
| Active power | $P_{r1}$ | 1021W |
| Reactive power | $Q_{r1}$ | 623var |
| Chain with Capacitors | | |
| Active power | $P_{r2}$ | 76W |
| Reactive power | $Q_{r2}$ | 2546var |

## VII. CONCLUSION

This paper has proposed a power distribution control for cascaded multilevel inverter with hybrid energy sources. A power distribution strategy between the energy storage elements and the capacitors has been developed and implemented by proposed control method. In this control method, the active power distribution between chains can be realized by active voltage vector superposition while the reactive power distribution can be achieved by initial operation point selection, and the energy storage elements provide all active power while the capacitors maintain DC voltage as well as exchange reactive power. Meanwhile, the stable operation region and the range of the initial operation point of proposed method have been derived by vector analysis. The experimental results have been shown to be consistent with simulation results and have confirmed the validity of the proposed power distribution control. Compared with the traditional active and reactive decoupling power distribution control method, the proposed control method in this paper has the advantages of fast dynamic response and simple implementation, it can be widely used in various cascaded multilevel hybrid systems.

## REFERENCES

[1] L. Wang, F. Bai, R. Yan, and T. K. Saha, "Real-time coordinated voltage control of PV inverters and energy storage for weak networks with high PV penetration," *IEEE Trans. Power Syst.*, vol. 33, no. 3, pp. 3383–3395, May 2018.

[2] J. Tan and Y. Zhang, "Coordinated control strategy of a battery energy storage system to support a wind power plant providing multi-timescale frequency ancillary services," *IEEE Trans. Sustain. Energy*, vol. 8, no. 3, pp. 1140–1153, Jul. 2017.

[3] J. I. Y. Ota, T. Sato, and H. Akagi, "Enhancement of performance, availability, and flexibility of a battery energy storage system based on a modular multilevel cascaded converter (MMCC-SSBC)," *IEEE Trans. Power Electron.*, vol. 31, no. 4, pp. 2791–2799, Apr. 2016.
[4] T. Soong and P. W. Lehn, "Evaluation of emerging modular multilevel converters for BESS applications," *IEEE Trans. Power Del.*, vol. 29, no. 5, pp. 2086–2094, Oct. 2014.
[5] E. Chatzinikolaou and D. J. Rogers, "A comparison of grid-connected battery energy storage system designs," *IEEE Trans. Power Electron.*, vol. 32, no. 9, pp. 6913–6923, Sep. 2017.
[6] L. Zhi-Bin, C. Yang, M. Qin-Dong, G. Hai-Feng, Z. Bai-hua, and L. Zhi-Gang, "Design of 2 MW/10 kV cascaded power conversion system," in *Proc. 40th Annu. Conf. IEEE Ind. Electron. Soc. (IECON)*, Oct./Nov. 2014, pp. 4250–4255.
[7] N. Kawakami *et al.*, "Development of a 500-kW modular multilevel cascade converter for battery energy storage systems," *IEEE Trans. Ind. Appl.*, vol. 50, no. 6, pp. 3902–3910, Nov./Dec. 2014.
[8] L. Maharjan, T. Yamagishi, H. Akagi, and J. Asakura, "Fault-tolerant operation of a battery-energy-storage system based on a multilevel cascade PWM converter with star configuration," *IEEE Trans. Power Electron.*, vol. 25, no. 9, pp. 2386–2396, Sep. 2010.
[9] W. Song and A. Q. Huang, "Fault-tolerant design and control strategy for cascaded H-bridge multilevel converter-based STATCOM," *IEEE Trans. Ind. Electron.*, vol. 57, no. 8, pp. 2700–2708, Aug. 2010.
[10] H. Salimian and H. Iman-Eini, "Fault-tolerant operation of three-phase cascaded H-bridge converters using an auxiliary module," *IEEE Trans. Ind. Electron.*, vol. 64, no. 2, pp. 1018–1027, Feb. 2017.
[11] S.-M. Kim, J.-S. Lee, and K.-B. Lee, "A modified level-shifted PWM strategy for fault-tolerant cascaded multilevel inverters with improved power distribution," *IEEE Trans. Ind. Electron.*, vol. 63, no. 11, pp. 7264–7274, Nov. 2016.
[12] M. Aleenejad, H. Mahmoudi, and R. Ahmadi, "Unbalanced space vector modulation with fundamental phase shift compensation for faulty multilevel converters," *IEEE Trans. Power Electron.*, vol. 31, no. 10, pp. 7224–7233, Oct. 2016.
[13] S. Vazquez, J. I. Leon, L. G. Franquelo, J. J. Padilla, and J. M. Carrasco, "DC-voltage-ratio control strategy for multilevel cascaded converters fed with a single DC source," *IEEE Trans. Ind. Electron.*, vol. 56, no. 7, pp. 2513–2521, Jul. 2009.
[14] H. Sepahvand, J. Liao, M. Ferdowsi, and K. A. Corzine, "Capacitor voltage regulation in single-DC-source cascaded H-bridge multilevel converters using phase-shift modulation," *IEEE Trans. Ind. Electron.*, vol. 60, no. 9, pp. 3619–3626, Sep. 2013.
[15] X. Zha, P. Wang, F. Liu, J. Gong, and F. Zhu, "Segmented power distribution control system based on hybrid cascaded multilevel converter with parts of energy storage," *IET Power Electron.*, vol. 10, no. 15, pp. 2076–2084, Dec. 2017.
[16] L. Liu, H. Li, S.-H. Hwang, and J.-M. Kim, "An energy-efficient motor drive with autonomous power regenerative control system based on cascaded multilevel inverters and segmented energy storage," *IEEE Trans. Ind. Appl.*, vol. 49, no. 1, pp. 178–188, Jan./Feb. 2013.
[17] W. Jiang *et al.*, "Flexible power distribution control in an asymmetrical-cascaded-multilevel-converter-based hybrid energy storage system," *IEEE Trans. Ind. Electron.*, vol. 65, no. 8, pp. 6150–6159, Aug. 2018.
[18] Q. Zhang, "Control of PV battery hybrid system using cascaded H bridge converter," in *Proc. IEEE 3rd Int. Future Energy Electron. Conf. ECCE Asia (IFEEC-ECCE Asia)*, Jun. 2017, pp. 2008–2012.
[19] L. Maharjan, S. Inoue, H. Akagi, and J. Asakura, "State-of-charge (SoC)-balancing control of a battery energy storage system based on a cascade PWM converter," *IEEE Trans. Power Electron.*, vol. 24, no. 6, pp. 1628–1636, Jun. 2009.
[20] Z. Liu, B. Liu, S. Duan, and Y. Kang, "A novel DC capacitor voltage balance control method for cascade multilevel STATCOM," *IEEE Trans. Power Electron.*, vol. 27, no. 1, pp. 14–27, Jan. 2012.
[21] Z. Chunyan and L. Zhao, "Advanced compensation mode for cascade multilevel static synchronous compensator under unbalanced voltage," *IET Power Electron.*, vol. 8, no. 4, pp. 610–617, Apr. 2015.
[22] Y. Shi, B. Liu, Y. Shi, and S. Duan, "Individual phase current control based on optimal zero-sequence current separation for a star-connected cascade STATCOM under unbalanced conditions," *IEEE Trans. Power Electron.*, vol. 31, no. 3, pp. 2099–2110, Mar. 2016.

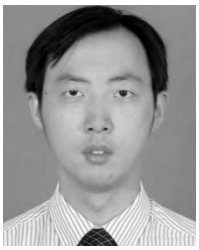

**ZHAO LIU** was born in Hubei, China, in 1983. He received the B.S. and Ph.D. degrees in electrical engineering from the Huazhong University of Science and Technology, Wuhan, China, in 2004 and 2010, respectively.

He is currently an Associate Professor with the School of Automation, Nanjing University of Science and Technology. His research interests include renewable energy applications, multilevel converters, and power electronics applied to power systems.

**YUE ZHANG** was born in Shaanxi, China, in 1995. He received the B.S. degree in smart grid from the Nanjing University of Science and Technology, Nanjing, China, in 2017.

He is currently pursuing the master's degree in control theory and control engineering with the School of Automation, Nanjing University of Science and Technology. His research interests include renewable energy applications and multilevel converters.

**SHANSHAN ZHAO** was born in Anhui, China, in 1995. She received the B.S. degree in smart grid from the Nanjing University of Science and Technology, Nanjing, China, in 2017.

She is currently pursuing the master's degree in power system and automation with the School of Automation, Nanjing University of Science and Technology. Her research interests include energy Internet and power electronics applied to power systems.

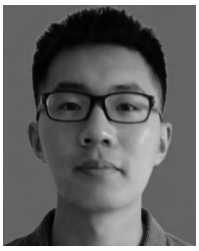

**JIAN GONG** was born in Anhui, China, in 1996. He received the B.S. degree in electrical engineering from the Nanjing University of Science and Technology, Nanjing, China, in 2018.

He is currently pursuing the master's degree with the School of Automation, Nanjing University of Science and Technology. His research interests include inverter paralleling and power electronics applied to power systems.